mize the single-particle spacing such that we could neglect transport through excited states.
11. The elastic current is given by the formula $I_{el}(\varepsilon) = eT_c^2\Gamma_R/[T_c^2(2 + \Gamma_R/\Gamma_L) + \Gamma_R^2/4 + (\varepsilon/h)^2]$; see Yu. V. Nazarov, *Phys. B* **189**, 57 (1993); T. H. Stoof and Yu. V. Nazarov, *Phys. Rev. B* **53**, 1050 (1996).
12. N. C. van der Vaart *et al.*, *Phys. Rev. Lett.* **74**, 4702 (1995).
13. Also, cotunneling can give excess current for $\varepsilon \neq 0$. In our measurements, however, the cotunneling current was less than 0.01 pA and can be neglected. For a review on cotunneling, see D. V. Averin and Yu. V. Nazarov, in (*3*), pp. 217–247.
14. A. J. Legget *et al.*, *Rev. Mod. Phys.* **59**, 1 (1987).
15. A T_c^2 dependence can also be obtained from perturbation theory when $T_c \ll \varepsilon$ [L. I. Glazman and K. A. Matveev, *Sov. Phys. JETP* **67**, 1276 (1988)].
16. We have reported a coherent coupling effect in double quantum dots using photon-assisted tunneling experiments [T. H. Oosterkamp *et al.*, *Nature*, in press]. These observations were made when a small bias voltage was applied. In this case, emission processes do not give rise to current.
17. Stimulated emission into the electromagnetic environment does play an important role for the presence of charging effects in single tunnel junctions [T. Holst *et al.*, *Phys. Rev. Lett.* **73**, 3455 (1994)].
18. Y. Nakamura, C. D. Chen, J. S. Tsai, *Phys. Rev. Lett.* **79**, 2328 (1997).
19. Bosonic excitations in a Fermi liquid (particle-hole excitations) can also be described as a bosonic bath with ohmic dissipation. For this case, the inelastic rate has a power-law dependence, $\Gamma(\varepsilon) \sim \varepsilon^{\gamma}$, where γ is related to the phase shift, δ, at the Fermi surface through $\gamma = 4/\pi^2\delta^2 - 1$ [see (*14*) and F. Guinea *et al.*, *Phys. Rev. B* **32**, 4410 (1985)]. Because $\delta^2 > 0$, the power $\gamma > -1$. This does not agree with our observed energy dependence, which is between $1/\varepsilon$ and $1/\varepsilon^2$.
20. We used a cylindrical cavity (diameter = 36 mm and height = 84 mm), which has a minimum resonance energy of about 20 μeV, and a rectangular cavity (22 mm by 19 mm by 8 mm) with resonance frequency of about 40 μeV.
21. Coupling to optical phonons is efficient only at much larger energies.
22. U. Bockelmann, *Phys. Rev. B* **50**, 17271 (1994).
23. For phonons, the inelastic rate at $T = 0$ can be written as $\Gamma_i \sim (T_c/\varepsilon)^2 J(\varepsilon)$, where $J(\varepsilon) \sim c^2(\varepsilon)g(\varepsilon)/\varepsilon$ is the spectral function and $c(\varepsilon)$ is the energy-dependent coupling (*14*). The phonon density of states $g(\varepsilon) \sim \varepsilon^{D-1}$ (D stands for dimension) such that $\Gamma_i \sim T_c^2 c^2(\varepsilon)\varepsilon^{D-4}$. When we neglect possible fine structure in $c(\varepsilon)$, we have for deformation $c \sim \varepsilon$ and thus $\Gamma_i \sim \varepsilon^{D-2}$, whereas for piezoelectric interaction c is constant and thus $\Gamma_i \sim \varepsilon^{D-4}$.
24. A. N. Cleland and M. L. Roukes, *Nature* **392**, 160 (1998).
25. J. M. Shilton *et al.*, *J. Phys. Condens. Matter* **8**, L531 (1997).
26. We thank M. Devoret, L. Glazman, S. Godijn, Y. Hirayama, J. Mooij, Yu. Nazarov, Y. Tohkura, N. Uesugi, M. Uilenreef, and N. van der Vaart for help and discussions. Supported by the Dutch Foundation for Fundamental Research on Matter (FOM) and L.P.K. by the Royal Netherlands Academy of Arts and Sciences.

28 July 1998; accepted 1 October 1998

Heterocyst Pattern Formation Controlled by a Diffusible Peptide

Ho-Sung Yoon and James W. Golden*

Many filamentous cyanobacteria grow as multicellular organisms that show a developmental pattern of single nitrogen-fixing heterocysts separated by approximately 10 vegetative cells. Overexpression of a 54–base-pair gene, *patS*, blocked heterocyst differentiation in *Anabaena* sp. strain PCC 7120. A *patS* null mutant showed an increased frequency of heterocysts and an abnormal pattern. Expression of a *patS-gfp* reporter was localized in developing proheterocysts. The addition of a synthetic peptide corresponding to the last five amino acids of PatS inhibited heterocyst development. PatS appears to control heterocyst pattern formation through intercellular signaling mechanisms.

The regulation of cell fate and pattern formation is a fundamental problem in developmental biology. Cell-cell communication often plays a key role in controlling development. Diffusible molecules that directly influence cell fate determination have been found in several eukaryotic organisms (*1*). Prokaryotic development in *Bacillus*, *Streptomyces*, and *Myxococcus* is also controlled by intercellular signaling (*2*, *3*). We have investigated the regulation of cell fate determination and pattern formation in a prokaryote that grows as a simple multicellular organism.

When the filamentous cyanobacterium *Anabaena* sp. strain PCC 7120 grows diazotrophically, approximately every tenth vegetative cell terminally differentiates into a heterocyst (*4*) (Fig. 1, A and B). This simple, one-dimensional developmental pattern spatially separates two incompatible processes: oxygen-evolving photosynthesis in vegetative cells and oxygen-sensitive nitrogen fixation in heterocysts. We have found that a small gene, *patS*, is crucial for the formation and maintenance of a normal heterocyst pattern.

The *patS* gene was identified on the conjugal cosmid 8E11 (*5*), which suppressed heterocyst development (Fig. 2A). A 3.3-kb subclone (pAM1035) was shown to confer the heterocyst-suppression phenotype (Het^s), and its sequence was determined (GenBank accession number AF046871). The same fragment isolated from an independent cosmid, 13C12, produced the same phenotype, indicating that the dominant Het^s phenotype is a property of wild-type sequences. An analysis of subcloned fragments in shuttle vectors (Fig. 2A) prompted us to investigate a small, 51–base pair (bp), open reading frame (ORF) named *patS* (Fig. 2B).

A 140-bp polymerase chain reaction (PCR) fragment containing the *patS* ORF (pAM1686) conferred the Het^s phenotype (Fig. 2A). Overexpression of *patS* by the *Anabaena* PCC 7120 *glnA* promoter (pAM1691) completely blocked heterocyst formation (Figs. 1C and 2A). The antisense orientation (pAM1695) produced no noticeable phenotype. *patS* blocks development at an early stage because even the cryptic pattern of nonfluorescent cells, which is produced by some developmental mutants (*6*), was not observed.

To test whether different levels of transcription correlate with the degree of heterocyst inhibition, we placed *patS* under the control of the copper-inducible *petE* promoter (P_{petE}) (*7*) (Fig. 3A). Without the addition of $CuSO_4$, the strain containing P_{petE}-*patS* was wild type. As *patS* transcription was increased by the addition of $CuSO_4$, there was a corresponding decrease in the frequency of heterocysts. We observed no influence of $CuSO_4$ on heterocyst development when *patS* was cloned in the reverse orientation (Fig. 3A).

Mutations in *patS* resulted in a loss of the ability to suppress heterocysts. pAM1882 (Fig. 2A) was mutagenized and screened for plasmids that failed to suppress heterocysts (*8*). Four plasmids were identified, each with a missense mutation within *patS* (Fig. 2B).

patS potentially encodes a 17–amino acid peptide, starting at the first available ATG codon; however, other in-frame ATG and GTG codons are present. PatS has no homologs or sequence motifs in the databases. It contains a stretch of five hydrophobic amino acids in its NH_2-terminal half, and its COOH-terminal half is mostly hydrophilic.

A *patS-lacZ* translational fusion showed that *patS* is translated and developmentally regulated (*9*). β-galactosidase (β-Gal)–specific activity of the in-frame fusion (Fig. 2C) increased about threefold (to 6000 units) during the 6 hours after the heterocyst induction and then decreased to the preinduction level after 27 hours. A direct analysis of the *patS* message on RNA blots yielded similar results

Department of Biology, Texas A&M University, College Station, TX 77843–3258, USA.

*To whom correspondence should be addressed.

(*10*). The out-of-frame construct produced background levels of β-Gal.

Because many cell-cell signaling molecules in Gram-positive bacteria are peptides (*11*, *12*) and because a long-standing model for the control of the heterocyst pattern involves a diffusible inhibitor that is produced by proheterocysts (*4*), we suspected that *patS* might encode an exported signaling molecule. We were intrigued with the phosphate regulator (*phr*) genes from *Bacillus subtilis* (*13*) and with *phrC* in particular, which encodes the quorum-sensing pheromone competence and sporulation stimulating factor (CSF) (*3*). The CSF is an unmodified exported pentapeptide that is processed from the COOH-terminal end of a 40–amino acid precursor. These precedents, and the fact that the four *patS* missense mutations happened to be in the last five codons (Fig. 2B), led us to test a synthetic pentapeptide corresponding to the COOH-terminal end of PatS.

This pentapeptide, PatS-5 (RGSGR), inhibited heterocyst formation at submicromolar concentrations (Fig. 3B) (*14*). Two altered peptides had reduced activity: PatS-4 (GSGR), which contains the last four amino acids, and PatS-G4S (RGSSR), which contains a G to S substitution corresponding to a mutation that reduced *patS* activity (Fig. 2B) (*14*). A mixture of each amino acid (R, G, and S) present in PatS-5 had no effect on heterocyst formation (Fig. 3B) (*14*).

patS is required to inhibit heterocyst formation. A *patS* deletion strain, AMC451 (*15*), formed heterocysts on a nitrate-containing medium; the wild type does not produce heterocysts in this medium. Twenty-four hours after the nitrogen step-down, wild-type filaments formed a pattern of single heterocysts that were separated by 8 to 14 vegetative cells (Figs. 1B and 3D). AMC451 formed multiple contiguous heterocysts and short vegetative-cell intervals (Figs. 1D and 3E). In the experiment shown in Fig. 3, D and E, the wild type formed single heterocysts (100%), whereas AMC451 formed single (39%), double (55%), quadruple (3%), and sextuple (3%) heterocysts. Longer chains of up to 10 contiguous heterocysts were occasionally formed (Fig. 1D). The phenotype of the Δ*patS* mutant AMC451 was due to the loss of *patS* alone because AMC451 was complemented by *patS* that was introduced on plasmids pAM1882, pAM1835, and pAM1686.

Heterocyst formation of AMC451 was inhibited by exogenously added PatS-5, indicating a normal response to the pentapeptide (Fig. 3C); however, the pattern was still abnormal. The induction of AMC451 in the presence of 60 nM PatS-5 reduced the number of heterocysts to about wild-type levels (11%) but failed to restore a normal pattern (Fig. 3F). This is consistent with a model that requires a gradient of the PatS signal originating from proheterocysts.

Expressing *patS* in only proheterocysts suppressed the pattern defects of the Δ*patS* mutant AMC451 and indicated that PatS functions in a manner that is nonautonomous to the cell. The *hepA* promoter is induced in proheterocysts between 4.5 and 7 hours after the nitrogen

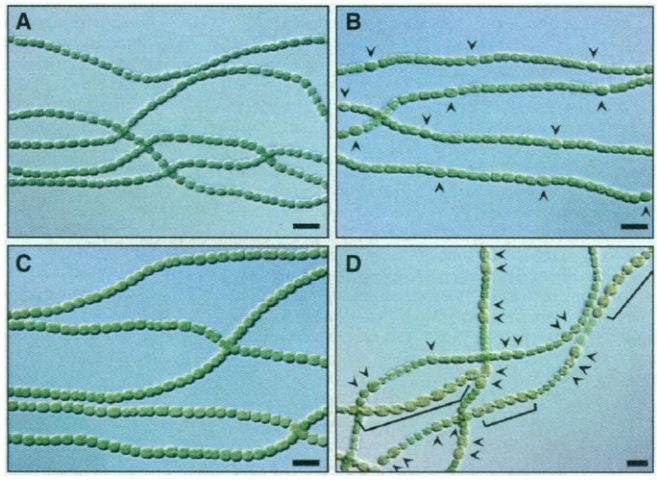

Fig. 1. *patS* controls heterocyst development in *Anabaena* PCC 7120. Wild-type filaments (**A**) grown in BG-11 medium and (**B**) after the nitrogen step-down in BG-11_0 to induce heterocysts (arrowheads) are shown. (**C**) Overexpression of *patS* from pAM1691 (Fig. 2A) prevented heterocyst formation in BG-11_0, and (**D**) deletion of *patS* (AMC451) resulted in supernumerary heterocysts with an abnormal pattern in BG-11_0. Brackets indicate chains of contiguous heterocysts. *Anabaena* PCC 7120 and derived strains were grown as previously described (*21*). Differential interference contrast micrographs were taken before (A) and 24 hours after (B through D) heterocyst induction. Scale bars, 10 μm.

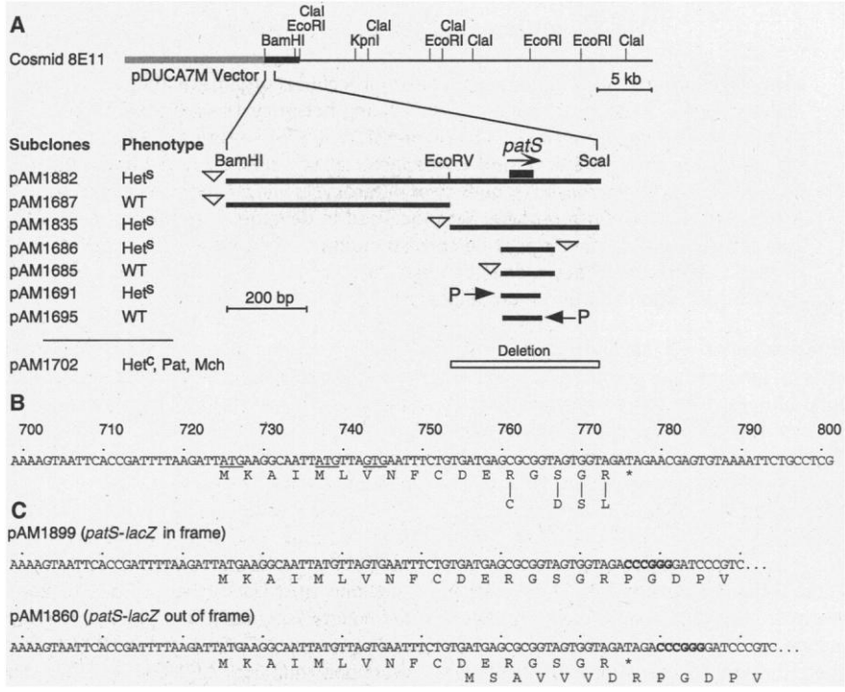

Fig. 2. (**A**) Identification of the *patS* gene on cosmid 8E11. Subclones were generated by cloning the indicated DNA fragments into shuttle vectors (*22*). The Bam HI–Cla I fragment in pAM1035 is indicated as a thick black bar on the 8E11 map. Cloning and molecular techniques were performed as previously described (*23*). Plasmids were transferred into *Anabaena* PCC 7120 by conjugation from *Escherichia coli* (*19*, *24*). WT, wild type; Het^s, heterocyst suppression; Het^c, heterocyst formation on a nitrate-containing medium; Pat, abnormal heterocyst pattern; Mch, multiple contiguous heterocysts; inverted triangle, transcription terminator; P with arrow, external promoter. (**B**) Nucleotide sequence of the smallest tested DNA fragment that is sufficient to suppress heterocyst development and the deduced amino acid sequence of PatS (*14*). Potential start codons are underlined. The amino acids encoded by four missense mutants are shown below the wild-type sequence. Nucleotide numbering begins with the first nucleotide in pAM1882. (**C**) Sequences of in-frame and out-of-frame *patS-lacZ* translational fusions (*9*). The Sma I site used for the constructions is shown in bold.

step-down (*16*). AMC451 containing a plasmid-borne P_{hepA}-*patS* fusion had a nearly wild-type pattern (Fig. 3G). Promoterless *patS* failed to complement the Δ*patS* phenotype (Fig. 3H).

As predicted for a gene encoding a diffusible inhibitor that controls pattern, *patS* expression was highest in differentiating cells. A *patS* transcriptional fusion with green fluorescent protein (GFPmut2) (*17*) on a low copy number plasmid (pAM1951) was used as a reporter. Weak GFP fluorescence with no obvious pattern was found in nitrate-grown filaments (Fig. 4A). A distinct pattern of brightly fluorescent cells was formed within the 12 hours after induction, which is before proheterocysts could be identified. After 18 hours, strong GFP fluorescence was localized to differentiating proheterocysts. After filaments began diazotrophic growth, GFP fluorescence was strongest from single cells that were midway between two heterocysts, where a new heterocyst will form (Fig. 4B). A strain containing a vegetative cell–specific promoter fused to *gfp* showed fluorescence from only vegetative cells (Fig. 4C). A strain containing pAM1956, which carries promoterless *gfp*, had no detectable GFP fluorescence.

PatS seems to play a key role in heterocyst pattern formation by inhibiting the formation of adjacent heterocysts and by maintaining a minimum number of vegetative cells between heterocysts. The inhibition of neighboring cells by select differentiating cells (lateral inhibition) is an important mechanism of pattern formation in eukaryotic organisms (*18*). Because it takes ~20 hours for heterocysts to mature and begin supplying fixed nitrogen to the filament, a specialized early inhibitory signal is required to allow only a fraction of starving cells to terminally differentiate. The first cells to differentiate increase the production of PatS to inhibit neighboring cells from forming heterocysts. PatS-producing cells must themselves be refractory to the PatS signal. The mechanism of immunity is unknown, but would be expected to involve a cell-autonomous inhibition of self-signaling such as that proposed for PrgY in enterococcal conjugation (*11*).

The PatS signal is likely to be a processed COOH-terminal peptide that is confined to the periplasm of this Gram-negative cyanobacterium. There is no evidence of heterocyst inhibition between filaments in mixed cultures or by a conditioned medium from a

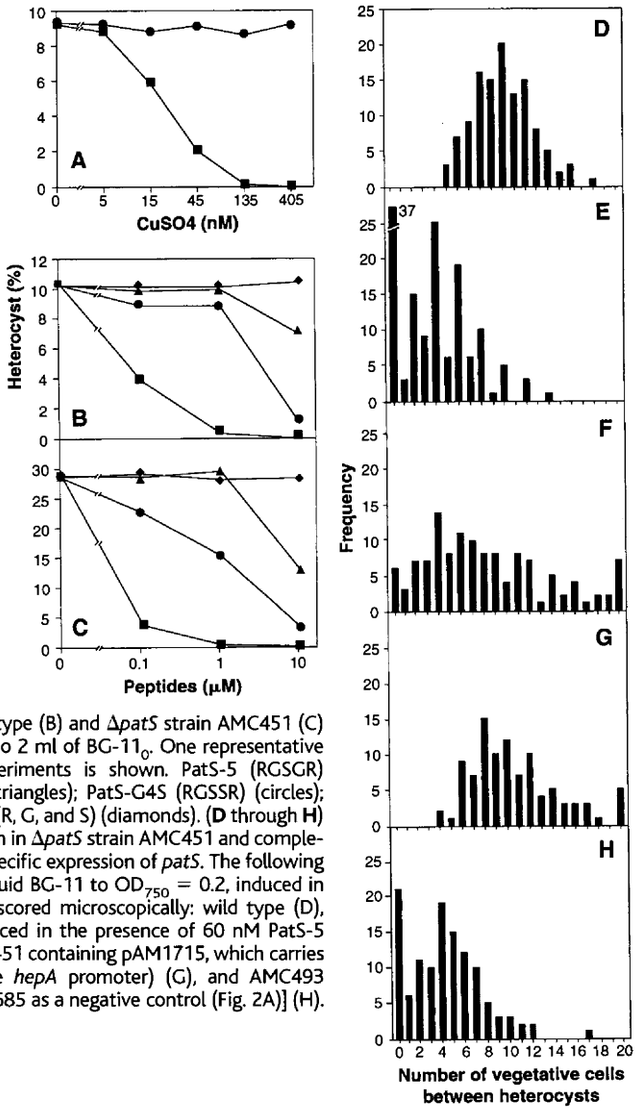

Fig. 3. (**A**) *patS* transcription suppressed heterocyst formation. Strains containing pAM1714 (squares), which carries P_{petE}-*patS*, or the control plasmid pAM1716 (circles) (*7*) were washed and grown for several generations in copper-free BG-11 liquid medium to deplete the residual copper. At an optical density of 750 nm (OD_{750}) = 0.4, cultures were induced by transferring the filaments to 2 ml of BG-11_0 that contained different concentrations of $CuSO_4$. The percentage of heterocysts was determined microscopically 24 hours after induction. At least 1000 cells were scored for each sample. Values are shown for one representative of four independent experiments. (**B** and **C**) Inhibition of heterocyst differentiation by synthetic peptides. Peptides (Genosys Biotechnologies, The Woodlands, Texas) were added to wild-type (B) and Δ*patS* strain AMC451 (C) immediately after transfer to 2 ml of BG-11_0. One representative of three independent experiments is shown. PatS-5 (RGSGR) (squares); PatS-4 (GSGR) (triangles); PatS-G4S (RGSSR) (circles); and mixture of amino acids (R, G, and S) (diamonds). (**D** through **H**) Abnormal heterocyst pattern in Δ*patS* strain AMC451 and complementation by heterocyst-specific expression of *patS*. The following filaments were grown in liquid BG-11 to OD_{750} = 0.2, induced in BG-11_0 for 24 hours, and scored microscopically: wild type (D), AMC451 (E), AMC451 induced in the presence of 60 nM PatS-5 peptide (F), AMC483 (AMC451 containing pAM1715, which carries *patS* that is driven by the *hepA* promoter) (G), and AMC493 [AMC451 containing pAM1685 as a negative control (Fig. 2A)] (H).

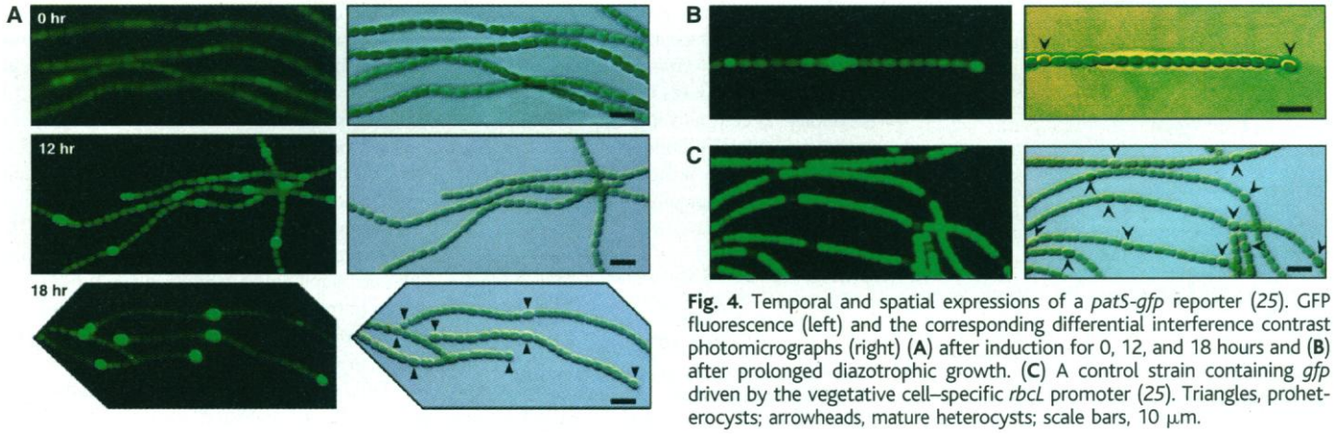

Fig. 4. Temporal and spatial expressions of a *patS-gfp* reporter (*25*). GFP fluorescence (left) and the corresponding differential interference contrast photomicrographs (right) (**A**) after induction for 0, 12, and 18 hours and (**B**) after prolonged diazotrophic growth. (**C**) A control strain containing *gfp* driven by the vegetative cell–specific *rbcL* promoter (*25*). Triangles, proheterocysts; arrowheads, mature heterocysts; scale bars, 10 μm.

strain overexpressing *patS* (*10*).

We propose a model in which a processed PatS peptide, originating from differentiating proheterocysts, diffuses along the filament's contiguous periplasmic space and is taken up by neighboring cells, creating a gradient of inhibitory signal. The intracellular target of PatS signaling is unknown, but components of a phosphorelay such as that found in *Bacillus* (*13*) are likely candidates.

References and Notes

1. D. S. Kessler and D. A. Melton, *Science* **266**, 596 (1994); K. Kornfeld, *Trends Genet.* **13**, 55 (1997); M. Freeman, *Development* **124**, 261 (1997).
2. H. B. Kaplan and L. Plamann, *FEMS Microbiol. Lett.* **139**, 89 (1996); J. R. Nodwell, K. McGovern, R. Losick, *Mol. Microbiol.* **22**, 881 (1996).
3. B. A. Lazazzera, J. M. Solomon, A. D. Grossman, *Cell* **89**, 917 (1997).
4. C. P. Wolk, A. Ernst, J. Elhai, in *The Molecular Biology of Cyanobacteria*, D. A. Bryant, Ed. (Kluwer Academic, Dordrecht, Netherlands, 1994), vol. 1, pp. 769–823.
5. C. C. Bauer *et al.*, *FEMS Microbiol. Lett.* **151**, 23 (1997); K. S. Ramaswamy, S. Endley, J. W. Golden, *J. Bacteriol.* **178**, 3893 (1996).
6. I. Khudyakov and C. P. Wolk, *J. Bacteriol.* **179**, 6971 (1997).
7. pAM1697 contains *patS* that was amplified by PCR and cloned into pPet1 (W. J. Buikema and R. Haselkorn, personal communication), which contains the *petE* promoter. pAM1714 contains the P_{petE}-*patS* fragment from pAM1697 in pAM504 (*19*). pAM1716 contains *patS* in the reverse orientation. Two independent clones for each construct were tested, and they produced similar results.
8. pAM1882 DNA (1 μg) was incubated in a final volume of 100 μl of 0.4 M hydroxylamine-HCl in buffer [50 mM sodium phosphate (pH 6.0) and 0.9 mM EDTA] at 65°C for 60 min [H. C. Lee, Y. P. Toung, Y. S. Tu, C. P. Tu, *J. Biol. Chem.* **270**, 99 (1995)]. After dialyzing the DNA against TE buffer [10 mM tris-HCl (pH 8.0) and 1 mM EDTA] overnight, 2 μl was used to transform *Escherichia coli* conjugal donor strain AM1359 (strain DH10B containing pRL623 and pRL443) [J. Elhai, A. Vepritskiy, A. M. Muro-Pastor, E. Flores, C. P. Wolk, *J. Bacteriol.* **179**, 1998 (1997)]. Several thousand transformant colonies were collected and used for conjugation with *Anabaena* PCC 7120. After incubating for 10 days on BG-11_0 plates containing neomycin (25 μg/ml), the four best-growing Het^+ exconjugants were selected for plasmid isolation and DNA sequencing.
9. In-frame (pAM1899) and out-of-frame (pAM1860) *patS-lacZ* translational fusions were made by ligating *patS* fragments to *lacZ*. *Anabaena* PCC 7120 exconjugants AMC446 (pAM1899) and AMC448 (pAM1860) were induced in BG-11_0 for 0, 6, 14, 18, 27, and 48 hours and harvested for β-Gal assays. Cells were lysed and assayed as previously described [M. R. Schaefer and S. S. Golden, *J. Bacteriol.* **171**, 3973 (1989)], except that the filaments were frozen at −85°C before processing. β-Gal was measured and expressed as specific activity (nanomoles of *o*-nitrophenyl-β-D-galactopyranoside per minute per milligram of protein).
10. H.-S. Yoon and J. W. Golden, data not shown.
11. G. M. Dunny and B. A. B. Leonard, *Annu. Rev. Microbiol.* **51**, 527 (1997).
12. M. Kleerebezem, L. E. Quadri, O. P. Kuipers, W. M. de Vos, *Mol. Microbiol.* **24**, 895 (1997).
13. M. Perego and J. A. Hoch, *Proc. Natl. Acad. Sci. U.S.A.* **93**, 1549 (1996); M. Perego, *ibid.* **94**, 8612 (1997).
14. Single-letter abbreviations for the amino acid residues are as follows: A, Ala; C, Cys; D, Asp; E, Glu; F, Phe; G, Gly; H, His; I, Ile; K, Lys; L, Leu; M, Met; N, Asn; P, Pro; Q, Gln; R, Arg; S, Ser; T, Thr; V, Val; W, Trp; and Y, Tyr.
15. AMC451 was made by double recombination with suicide plasmid pAM1702 (Fig. 2A) as previously described (*19*). pAM1702 contains *patS*-flanking sequences and an Ω Sp^r/Sm^r cassette (conferring spectinomycin and streptomycin resistance) in *sacB*-containing suicide vector pRL278 [T. A. Black, Y. Cai, C. P. Wolk, *Mol. Microbiol.* **9**, 77 (1993)]. The Ω Sp^r/Sm^r cassette replaces a 381-bp Eco RV–Sca I fragment containing the entire *patS* gene. Four independent isolates with identical phenotypes were obtained after selection on media containing sucrose (5%), spectinomycin (2 μg/ml), and streptomycin (2 μg/ml). The structure of the deletion was confirmed by Southern (DNA) blot analysis.
16. Y. Cai and C. P. Wolk, *J. Bacteriol.* **179**, 267 (1997).
17. B. P. Cormack, R. H. Valdivia, S. Falkow, *Gene* **173**, 33 (1996).
18. P. Simpson, *Development* **109**, 509 (1990).
19. T.-F. Wei, T. S. Ramasubramanian, J. W. Golden, *J. Bacteriol.* **176**, 4473 (1994).
20. T. S. Ramasubramanian, T.-F. Wei, J. W. Golden, *ibid.*, p. 1214.
21. J. W. Golden, L. L. Whorff, D. R. Wiest, *ibid.* **173**, 7098 (1991).
22. Details of plasmid constructions are available from the authors. Subclones were from pAM1035, which contains *patS* on a 3.3-kb Bam HI–Cla I fragment that was cloned into the same sites of pBluescript II KS(−). pAM1882, pAM1687, and pAM1835 contain restriction fragments in the conjugal shuttle vector pAM504 (*19*). pAM1685 contains *patS* that was amplified by PCR and cloned into pAM504. pAM1686 contains the same insert cloned into pAM505 (identical to pAM504 except that the Bam HI and Sac I sites are reversed). pAM1691 and pAM1695 contain *patS* cloned into pAM743, which contains the *Anabaena* PCC 7120 *glnA* promoter from pAM658 (*20*) in pAM504. The sequences of all inserts that were generated by PCR were confirmed after subcloning.
23. K. S. Ramaswamy, C. D. Carrasco, T. Fatma, J. W. Golden, *Mol. Microbiol.* **23**, 1241 (1997).
24. C. D. Carrasco, K. S. Ramaswamy, T. S. Ramasubramanian, J. W. Golden, *Genes Dev.* **8**, 74 (1994).
25. The *patS-gfp* transcriptional fusion in pAM1951 was made by first cloning a fragment containing 724 bp upstream of *patS* into pKEN2-GFPmut2 (*17*) to make pAM1877. A fragment containing *patS-gfp* from pAM1877 was ligated into pAM505 to make pAM1951. *gfp* from pKEN2-GFPmut2 was cloned into pAM542 (*20*), which contains P_{rbcL} on a shuttle vector, to make pAM1954. pAM1956 contains promoterless *gfp* from pKEN2-GFPmut2 inserted into pAM505.

26. We thank L. Whorff for contributions to the initial analysis of cosmid 8E11; A. Ott for technical assistance; and W. J. Buikema, J. Elhai, S. S. Golden, M. D. Manson, and members of our laboratory for critically reading the manuscript. Supported in part by NIH grant GM36890.

23 July 1998; accepted 29 September 1998

Binding of Hepatitis C Virus to CD81

Piero Pileri,* Yasushi Uematsu,* Susanna Campagnoli, Giuliano Galli, Fabiana Falugi, Roberto Petracca, Amy J. Weiner, Michael Houghton, Domenico Rosa, Guido Grandi, Sergio Abrignani†

Chronic hepatitis C virus (HCV) infection occurs in about 3 percent of the world's population and is a major cause of liver disease. HCV infection is also associated with cryoglobulinemia, a B lymphocyte proliferative disorder. Virus tropism is controversial, and the mechanisms of cell entry remain unknown. The HCV envelope protein E2 binds human CD81, a tetraspanin expressed on various cell types including hepatocytes and B lymphocytes. Binding of E2 was mapped to the major extracellular loop of CD81. Recombinant molecules containing this loop bound HCV and antibodies that neutralize HCV infection in vivo inhibited virus binding to CD81 in vitro.

HCV is a positive strand RNA virus of the flaviviridae family (*1*) chronically infecting about 170 million persons worldwide (*2*). Chronic HCV infection results in liver diseases (hepatitis, cirrhosis, and hepatocellular carcinoma) in a sizable fraction of cases (*3*). Infection with HCV is also associated with most cases of type II and type III cryoglobulinemia, B lymphocyte proliferative disorders characterized by polyclonal B cell activation and autoantibody production (*4*). The complete HCV sequence has been available since 1989 (*5*); however, progress in understanding the viral life cycle has been hampered by the lack of virus culture systems in vitro. Although hepatocytes and B lymphocytes are thought to be infected by HCV (*1*), there is no consensus on viral tropism, and the cellular receptor for the virus has not been identified.

We have shown previously that a recombinant form of the major envelope protein (E2) of HCV binds with high affinity to human lymphoma and hepatocarcinoma cell lines, whereas it does not bind to mouse cells (*6*). Furthermore, in chimpanzees vaccinated with recombinant E1 and E2 envelope proteins, protection from homologous HCV challenge correlated with the presence of antibodies capable of inhibiting the binding of E2 to human cells (*6*). These results suggested that E2 may be responsible for binding of HCV to target cells.

To identify the E2-binding molecule on human cells, we prepared a cDNA expression

P. Pileri, Y. Uematsu, S. Campagnoli, G. Galli, F. Falugi, R. Petracca, D. Rosa, G. Grandi, S. Abrignani, IRIS, Chiron, Siena 53100, Italy. A. J. Weiner and M. Houghton, Chiron Corporation, Emeryville, CA 94608, USA.

*These authors contributed equally to this work.
†To whom correspondence should be addressed. E-mail: abrignani@iris02.biocine.it